



**HAL**  
open science

## Statistical properties of ionospheric stimulated electromagnetic emissions

R. L. Karlsson, T. D. Carozzi, L. Norin, J. E. S. Bergman, B. Thidé

► **To cite this version:**

R. L. Karlsson, T. D. Carozzi, L. Norin, J. E. S. Bergman, B. Thidé. Statistical properties of ionospheric stimulated electromagnetic emissions. *Annales Geophysicae*, 2006, 24 (7), pp.1851-1859. hal-00318119

**HAL Id: hal-00318119**

**<https://hal.science/hal-00318119v1>**

Submitted on 18 Jun 2008

**HAL** is a multi-disciplinary open access archive for the deposit and dissemination of scientific research documents, whether they are published or not. The documents may come from teaching and research institutions in France or abroad, or from public or private research centers.

L'archive ouverte pluridisciplinaire **HAL**, est destinée au dépôt et à la diffusion de documents scientifiques de niveau recherche, publiés ou non, émanant des établissements d'enseignement et de recherche français ou étrangers, des laboratoires publics ou privés.

# Statistical properties of ionospheric stimulated electromagnetic emissions

R. L. Karlsson<sup>1</sup>, T. D. Carozzi<sup>2</sup>, L. Norin<sup>1</sup>, J. E. S. Bergman<sup>3</sup>, and B. Thidé<sup>3,4</sup>

<sup>1</sup>Department of Astronomy and Space Physics, Uppsala University, Box 515, SE-751 20 Uppsala, Sweden

<sup>2</sup>Space Science Centre, University of Sussex, Brighton, BN1 9QT, UK

<sup>3</sup>Swedish Institute of Space Physics, Uppsala, Box 537, SE-751 21 Uppsala, Sweden

<sup>4</sup>LOIS Space Centre, Växjö University, SE-35195 Växjö, Sweden

Received: 28 September 2005 – Revised: 5 June 2006 – Accepted: 8 June 2006 – Published: 9 August 2006

**Abstract.** We have analysed the statistical properties of the stimulated electromagnetic emissions (SEE) spectral features in the steady state, reached after a long period of continuous HF pumping of the ionosphere in experiments performed at the Sura ionospheric radio research facility in Russia. Using a digital filter bank method, we have been able to analyse complex valued signals within narrow frequency bands. Each of the SEE spectral features are thereby separated into a number of narrow spectral components. Statistical tests were performed for all these spectral components and the distributions of the spectral amplitudes and phases were evaluated. Also, a test for sinusoidal components was performed. These tests showed that all observed SEE features were indistinguishable from coloured Gaussian noise. The test results exclude that the SEE features can be the result of a single isolated coherent process, but does not rule out that there could be many statistically independent parametric wave-wave processes taking place simultaneously at various parts of the HF-pumped ionosphere, as long as the superposition from all these is incoherent. Furthermore, from the test results, we cannot exclude the possibility that the waveforms of some, or all, of the SEE features may be chaotic.

**Keywords.** Ionosphere (Active experiments; Ionospheric irregularities) – Space plasma physics (Wave-wave interactions)

## 1 Introduction

A powerful HF radio wave transmitted from the ground into the ionosphere at a frequency near a resonance frequency of the ionospheric plasma gives rise to secondary radiation from the ionosphere. This secondary radiation has a power spectral density (PSD) with weak, asymmetric, and richly struc-

tured sidebands around the injected radio frequency (Thidé et al., 1982). It has been given the name stimulated electromagnetic emissions (SEE) and has spectral and temporal characteristics which exhibit systematic and repeatable behaviour. A comprehensive description of SEE is given by Leyser (2001).

Most models for SEE (e.g. Stubbe et al., 1984; Thidé, 1990) are based on parametric processes, which are inherently phase coherent (Weiland and Wilhelmsson, 1977; Leyser, 2001). The decomposition products of these wave-wave interactions are strictly phase coupled to the pump wave. Since the pump itself is highly phase coherent, the SEE features should also show a high degree of coherency if they are to be explained purely by parametric processes. However, from the PSD alone it is not clear whether the spectral SEE features correspond to coherent or noise-like processes. To answer this question we have analysed the amplitude and phase distributions of the spectral SEE features and also considered their first order statistics.

## 2 Hypothesis

A simple model for a deterministic signal is a superposition of sinusoidal modes with well defined amplitudes and phases. Therefore, we apply a sum-of-sines model with the calculation of a windowed Fourier transform and the use of a digital filter bank approach. The filter bank contains all the narrow frequency bins obtained from the Fourier transform and here the term spectral component refers to these narrow frequency bands. The Fourier transform resolution is chosen such that the SEE features span over many spectral components. Background noise is also present during the measurements and the data can therefore be considered as weakly deterministic. Furthermore, after several seconds of continuous pumping of the ionosphere, the statistics for

---

Correspondence to: R. L. Karlsson  
(rk@irfu.se)

the PSD do not change over time and the SEE is said to be in steady-state.

Most basic SEE models are based on parametric decay processes, which conserve energy and momentum. For a three-wave decay process, the conservation of energy and momentum implies that

$$\omega_{\text{mother}} = \omega_{\text{daughter}_1} + \omega_{\text{daughter}_2} \quad (1)$$

$$\mathbf{k}_{\text{mother}} = \mathbf{k}_{\text{daughter}_1} + \mathbf{k}_{\text{daughter}_2}. \quad (2)$$

Letting  $\phi$  denote the phase of a wave, we have (Whitham, 1974)

$$\omega = -\frac{\partial \phi}{\partial t} \quad (3)$$

$$\mathbf{k} = \nabla \phi. \quad (4)$$

This implies that the total phase also is conserved for the interaction:

$$\phi_{\text{mother}} = \phi_{\text{daughter}_1} + \phi_{\text{daughter}_2}. \quad (5)$$

In other words, if the pump wave is monochromatic and phase coherent, the decay products should also be phase coherent.

We investigate whether the SEE features are coherent and can be described as a sum-of-sines with additive noise. A sinusoidal gives rise to a DC component of the amplitude and the amplitude distributions of noise added sinusoidal signals follow Rice distributions (Rice, 1944). On the other hand, if no sinusoidal components are present we have narrowband, or coloured, Gaussian noise with Rayleigh distributed amplitudes of zero mean value and uniformly distributed phases (Bendat and Piersol, 1971).

The statistical properties can be used to assess the stochastic/deterministic nature of the SEE features. This has been done in the form of a number of statistical tests, where we expect to reject the null hypothesis:

**Null Hypothesis ( $H_0$ ).** *SEE is coloured complex Gaussian noise.*

In other words,  $H_0$  states that the complex amplitudes in narrow frequency bands of the SEE spectrum do not contain any DC components and are the results of a narrowband complex Gaussian process.

According to  $H_0$ , the SEE spectral amplitudes should be Rayleigh distributed while the phases should be uniformly distributed (Bendat and Piersol, 1971). In order to validate  $H_0$ , we perform a number of tests. In the first two tests we investigate the amplitude and phase distributions and compare with the distributions of narrowband Gaussian noise.

**Test 1 ( $T_1$ ).** *Test for the distribution of the spectral component amplitudes.*

In this test a comparison between the amplitude distribution of the spectral SEE features and the Rayleigh distribution is made.

**Test 2 ( $T_2$ ).** *Test for the distribution of the spectral component phases.*

Here the phase distribution of the spectral SEE features are compared with the uniform distribution.

We reject  $H_0$  if the SEE spectral component amplitudes are not Rayleigh distributed or if the SEE spectral component phases are not uniformly distributed. In that case we suspect that the SEE features contain a DC component and coloured complex Gaussian noise, but to insure that the DC component is present, a third test for sinusoidal components must be undertaken.

**Test 3 ( $T_3$ ).** *Test for sinusoidal components.*

Sinusoidal components give rise to a non-zero mean value of the spectral component amplitudes and we test the data for a zero mean value.

Under the assumption that  $T_1$  has shown that the spectral component amplitudes of the SEE features are not Rayleigh distributed, we have two possibilities. Either,  $T_3$  shows presence of sinusoidals which implies that the amplitudes are Rice distributed (Rice, 1944), or  $T_3$  does not show any sign of sinusoidals and the amplitudes have an unknown distribution. If, on the other hand,  $T_1$  and  $T_2$  show that the spectral components of the SEE features cannot be distinguished from narrowband Gaussian noise, i.e.,  $H_0$  can not be rejected, the outcome of  $T_3$  is irrelevant.

Radio interferences are present in most SEE data. These man-made signals should be different from noise. Consequently, we expect them to show deviations from the spectral amplitude and phase distributions of coloured complex Gaussian noise.

### 3 Method

In order to test the statistical hypotheses of the spectral SEE features, we have performed in total three goodness-of-fit tests. The first test  $T_1$  is a  $\chi^2$  test to investigate the similarity between the measured amplitude distributions and the Rayleigh distribution. The second test  $T_2$  is also a  $\chi^2$  test investigating if the phases are uniformly distributed. Finally, a Fisher's test  $T_3$  is performed to examine if the spectral components contain sinusoidals.

#### 3.1 Filter bank

The analysed complex valued SEE data  $x(t)$  were divided into  $M$  non-overlapping segments of  $L=1024$  samples. For each of these segments, a windowed Fourier transform was calculated using the von Hann (Hanning) window. Thereby 1024 spectral components were formed and these make up the filter bank. Defining  $s=Lf/f_S$  as the frequency index or spectral index,  $\tau=tf_S$  as the time index,  $f_S$  as the sampling

frequency, and  $h$  as the temporal window function, the windowed Fourier transform becomes

$$X_\tau(s) = \frac{\sum_{l=1}^L x(\tau + l)h(l)e^{-i2\pi sl/L}}{\sqrt{\sum_{l=1}^L |h(l)|^2}}. \quad (6)$$

The windowed Fourier transform is used in the statistical analysis of the spectral amplitudes and spectral phases. Implementing no overlap, the number of independent estimates  $M$  per spectral component is equal to the total data length divided by  $L$ .

By squaring  $X_\tau(s)$  and averaging over all the  $M$  estimates, an essentially noise free power spectrum is obtained:

$$\bar{S}(s) = \frac{1}{M} \sum_{\tau=1}^M |X_\tau(s)|^2. \quad (7)$$

Historically, for convenience and simplicity, the spectral properties of the SEE data have been represented in terms of the power spectrum or the PSD. Here the power spectrum of Eq. (7) will be used to visualise the SEE features.

### 3.2 $T_1$ : Test for the distribution of the spectral component amplitudes

According to  $H_0$ , no DC component is present and the spectral amplitudes should have zero mean value and be Rayleigh distributed. In presence of sinusoids, the amplitudes have a non-zero mean value and do not follow a Rayleigh distribution. By performing  $T_1$ , we expect to show that the spectral amplitudes are not Rayleigh distributed so that  $H_0$  can be rejected, with implication that the SEE features are statistically different from coloured complex Gaussian noise.

In order to put spectral amplitudes of different power on an equal footing, the data was normalised by dividing each spectral amplitude with the square root of its time-average power as given by Eq. (7). For each spectral component, the normalised spectral amplitudes were then binned into a histogram with linear spacing.

Let  $p_{r,n}$  denote the probability that an amplitude belonging to a Rayleigh distribution will show up in bin  $n$ . Then the product  $Mp_{r,n}$  represents the total number of amplitudes in bin  $n$ . The limits of the first and last bins has been chosen so that the number of amplitudes in the outer bins is slightly higher than five. For smaller values than five, the  $\chi^2$  test will give a misleading result. In total, 101 bins were used and the first  $N=100$  bins were intended for the useful data, while the highest bin was used to collect all the large amplitudes of low probability which were excluded from the test.

For a spectral index  $s$ , we denote the number of amplitudes within bin  $n$  by  $A_n(s)$  and the  $\chi^2$  spectral amplitude test parameter becomes

$$Q_A(s) = \sum_{n=1}^{N=100} \frac{[A_n(s) - Mp_{r,n}(s)]^2}{Mp_{r,n}(s)}, \quad (8)$$

where  $M$  is the total number of estimates per spectral component, and  $Mp_{r,n}(s)$  denotes the number of amplitudes in bin  $n$  as predicted by the normalised Rayleigh distribution. The test parameter  $Q_A(s)$  is  $\chi^2$  distributed with 99 deg of freedom.

### 3.3 $T_2$ : Test for the distribution of the spectral component phases

The expected result of  $T_2$  is that the spectral component phases of the SEE features are not uniformly distributed in time so that  $H_0$  can be rejected.

In this case it is not necessary to normalise the data. Instead we add a phase shift corresponding to the total phase shift measured from the start of the time series. After that, the corrected phases were, for each spectral component, binned into a histogram of  $N=100$  bins between the outer limits  $\pm\pi$ . Let  $p_{u,n}$  denote the probability that a uniformly distributed phase will show up in bin  $n$  and let  $P_n(s)$  denote the number of spectral phases in bin  $n$ . Then the  $\chi^2$  phase test parameter becomes

$$Q_P(s) = \sum_{n=1}^{N=100} \frac{[P_n(s) - Mp_{u,n}(s)]^2}{Mp_{u,n}(s)}, \quad (9)$$

where  $M$  is the total number of estimates per spectral component, and  $Mp_{u,n}(s)$  denotes the expected number of spectral components in bin  $n$  according to the uniform distribution. The phase test parameter  $Q_P(s)$  is  $\chi^2$  distributed with 99 deg of freedom.

### 3.4 $T_3$ : Test for sinusoidal components

Test  $T_1$  examined whether the spectral component amplitudes were Rayleigh distributed. If a deviation from the Rayleigh distribution is found, the spectral component amplitudes should contain sinusoids, which is indicated by a non-zero mean value. In  $T_3$ , the mean value is tested. This is done by studying the first order spectrum, which is the mean value of the spectral amplitudes. Expressed in power units, the first-order spectrum is

$$\bar{S}_m(s) = \frac{1}{M} \left| \sum_{\tau=1}^M X_\tau(s) \right|^2. \quad (10)$$

The test parameter has been chosen as the quotient of the first to the second order spectrum. With the second order spectrum given by Eq. (7), the Fisher's test parameter becomes

$$f(s) = \frac{\left| \sum_{\tau=1}^M X_\tau(s) \right|^2}{\sum_{\tau=1}^M |X_\tau(s)|^2} \quad (11)$$

which is  $F$  distributed with 2 and  $2M-2$  deg of freedom (Percival and Walden, 1993, p. 499; Thomson, 1982).

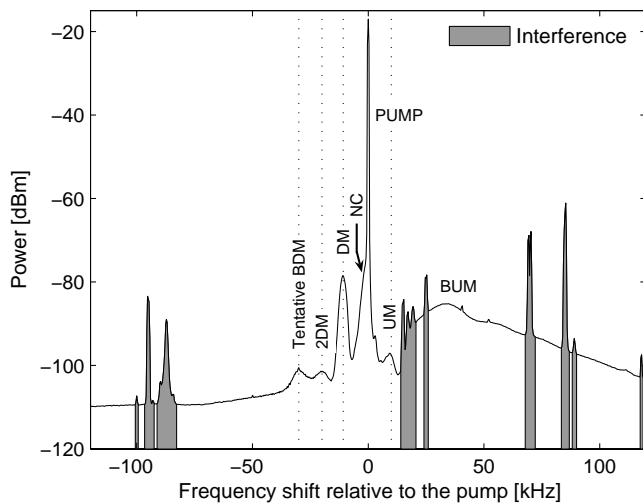


**Fig. 1.** The SEE spectrum with the visible SEE components indicated. Interferences from other radio sources are marked by shading. The data was taken at the Sura ionospheric HF pumping facility, Russia at 15:46 LT on 22 September 1998.

#### 4 Experiment and data

The data we have analysed was measured at the Sura ionospheric HF pumping facility, close to Vasil'sursk, Russia on 22 September 1998. The receiving antenna was directly coupled to an Hewlett Packard E1437A VXI digitiser without any filters or amplifiers in between. The HP E1437A provides up to 23 bits linear sampling at 20 Msamples/s, performs digital down-conversion, and outputs complex valued signals (I and Q) in calibrated units.

In this paper, we present data captured at 15:46 LT. During the experiment, the pump was turned on for 60 s at 6760 kHz in O mode and injected vertically into the overdense plasma of the ionosphere. We have omitted the first 12.5 s after pump onset, thus allowing the SEE features time to reach a steady state. In total, about 12 million samples at a base-band sampling rate of 320 kHz were used. With a filter bank of  $L=1024$  spectral components, the total number of samples gives  $M=11\,718$  independent estimates per spectral component.

Using Eq. (7), the time-averaged power spectrum can be calculated for the data as it is shown in Fig. 1. The pump and some of the SEE features (Leyser, 2001), such as the broad upshifted maximum (BUM), upshifted maximum (UM), narrow continuum (NC), downshifted maximum (DM), and second downshifted maximum (2DM) are indicated in Fig. 1. The figure also shows a structure at  $-30$  kHz which is where the broad downshifted maximum (BDM) may appear. This structure does not have exactly the shape we would expect from the BDM and in the following we will denote it tentative BDM. The tentative BDM is most likely instrument driven and will be discussed in more detail in Sect. 6.2.

Interferences originating from other radio sources are indicated by shading in Fig. 1. Since the interferences are of approximately the same intensity as the SEE features, it is illustrative to use them for comparison.

#### 5 Results

The probability density of observing a certain amplitude is shown in Fig. 2. Most of the spectral components show distributions close to a Rayleigh distribution. This is particularly clear in the figure for the frequency  $-120$  kHz, which describes an almost perfect Rayleigh distribution. Some spectral components seem to deviate from the Rayleigh distribution. This is the case for the interferences marked in Fig. 1, the pump wave, and the tentative BDM. Comparisons with the Rayleigh distribution are shown in detail for spectral components of the DM, the pump wave, and the tentative BDM in Figs. 3, 4, and 5, respectively. In these figures, the amplitude distributions are plotted with solid lines and the Rayleigh distributions with dashed lines. Visually, the DM appears to be Rayleigh distributed while the amplitudes of the pump and the tentative BDM seem to deviate from a Rayleigh distribution. The BUM, UM, NC, and 2DM all show distributions similar to the DM.

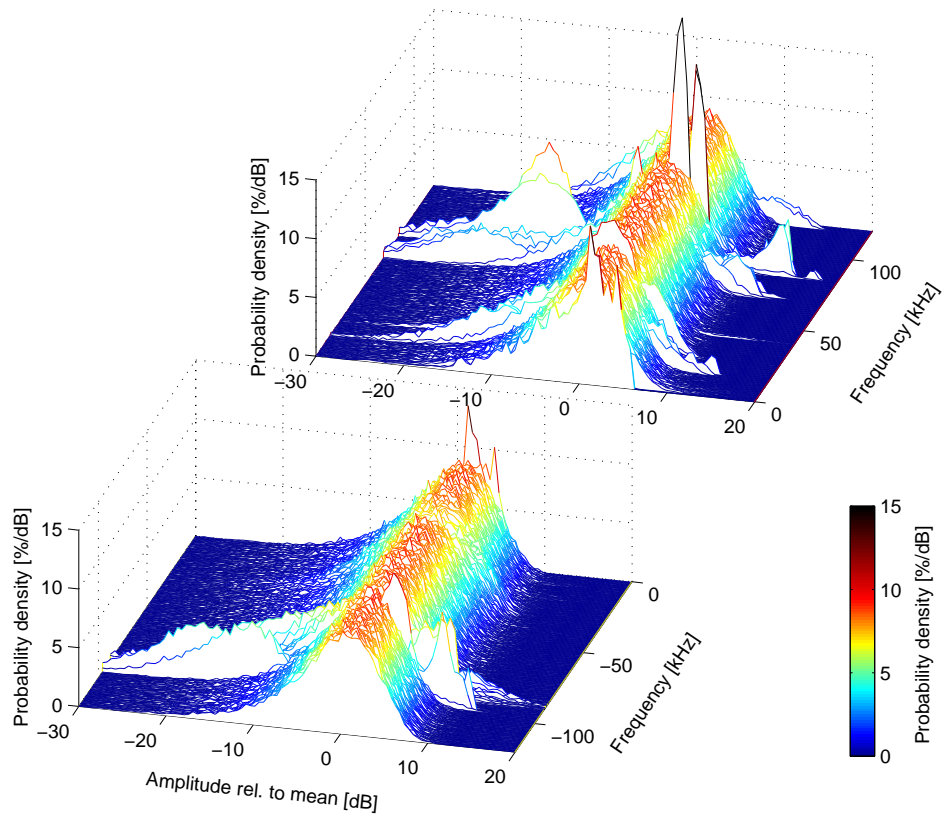
##### 5.1 Test analysis

While Figs. 2–5 only give indications about the shapes of the amplitude distributions, the goodness-of-fit tests provide a more precise answer. The value of the  $\chi^2$  test parameters are shown in Figs. 6a and 6b. Figure 6a displays the spectral amplitude test parameter of  $T_1$  and Fig. 6b the spectral phase test parameter of  $T_2$ . In Fig. 6c, the SEE power spectrum is shown. The vertical dotted lines are the same as in Fig. 1 and have been drawn to make it easy to identify the test parameters of the SEE features.

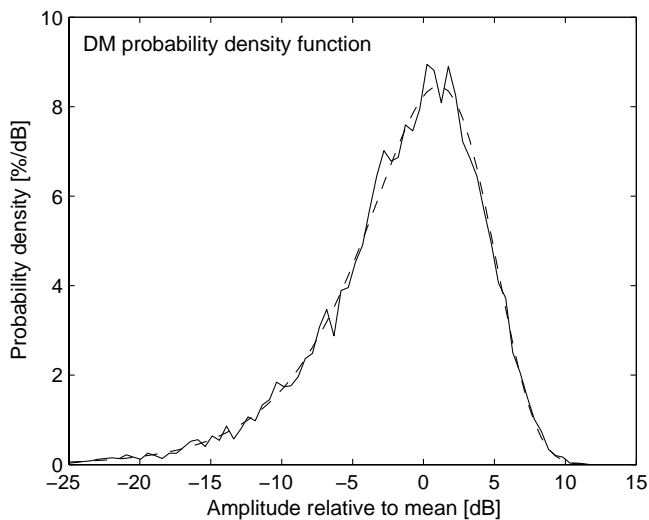
In both tests, the test parameters are  $\chi^2$  distributed with 99 degrees of freedom. The  $p$  values of 5%, 0.1%, and  $10^{-4}\%$  have been plotted in Figs. 6a and 6b. These correspond to values of the test parameter given by  $\chi_{0.05}^2(99)=123$ ,  $\chi_{0.001}^2(99)=148$ , and  $\chi_{10^{-6}}^2(99)=181$ , respectively. The meaning of a  $p$  value of, for example, 0.1% is that with a probability of 99.9%, values exceeding  $\chi_{0.001}^2(99)$  are not noise.

Figure 7 shows the sinusoidal component test or Fisher's test  $T_3$ . The first order spectrum given by Eq. (10) is shown in Fig. 7a, where the presence of noise makes it hard to identify the SEE features. These features are much clearer in the smooth second order spectrum, the average power spectrum, shown in Fig. 7b (and Figs. 1 and 6c), which has been formed by averaging  $M=11\,718$  spectra and thereby effectively removing the noise.

The result of the sinusoidal components test  $T_3$  is displayed in Fig. 7c, showing the test parameter  $f(s)$  given by Eq. (11). Lines corresponding to  $p$  values of 5%,



**Fig. 2.** The probability of measuring a certain spectral amplitude is shown in percent per dB for the same data as in Fig. 1. In the upper panel, positive frequency shifts relative to the pump wave are displayed, while the lower panel displays negative frequency shifts. In order to clearly visualise both small and large values of the spectral amplitudes, a logarithmic scale has been chosen and the spectral amplitudes are given in dB relative to their time-average.



**Fig. 3.** Comparison between the measured amplitude distribution of the DM (solid line) and the Rayleigh distribution (dashed line). The same axes as in Fig. 2 have been used.

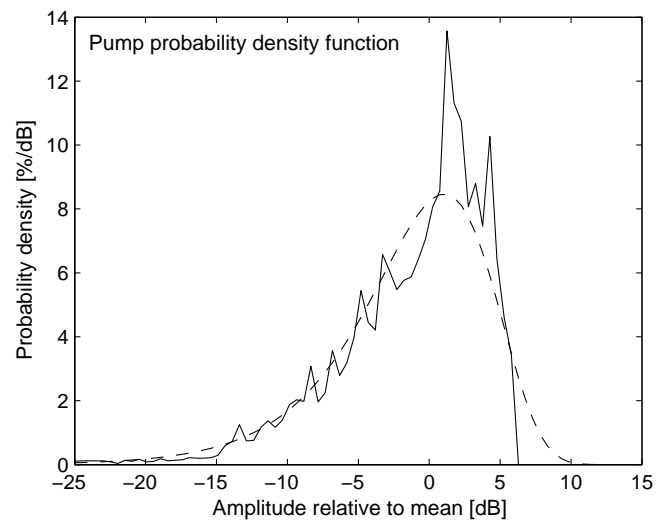


**Fig. 4.** Comparison between the measured amplitude distribution of the pump (solid line) and the Rayleigh distribution (dashed line). The axes are the same as in Fig. 2.

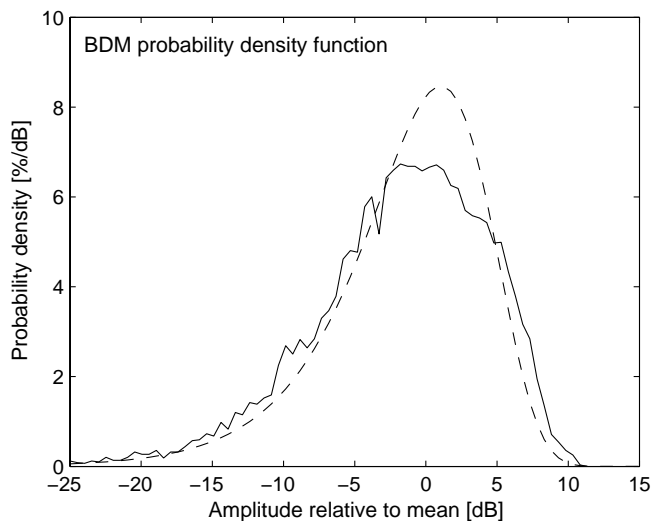


**Fig. 5.** Comparison between the measured amplitude distribution of the tentative BDM (solid line) and the Rayleigh distribution (dashed line). The axes are the same as in Fig. 2.

0.1%, and  $10^{-4}\%$  has also been plotted. These corresponds to values of the test parameter given by the  $F$ -distribution:  $F_{0.05}(2,2M-2)=3.0$ ,  $F_{0.001}(2,2M-2)=6.9$ ,  $F_{10^{-6}}(2,2M-2)=13.8$ , respectively. Spectral components with a test parameter larger than, e.g.,  $F_{0.001}(2,2M-2)$  is within 99.9% certainty not noise. Figure 7c shows that the two largest peaks of the test parameter are the pump and the interference at  $-95$  kHz. Four other peaks reach above the  $p=0.1\%$  level, but none of them match any SEE feature even though one peak lies between the DM and the 2DM. These four peaks are small compared to the two largest peaks and at least one of them should correspond to the 0.1% of the frequencies expected to reach above this level.

## 6 Discussion

### 6.1 The SEE features

In Figs. 6a and b, the SEE features BUM, UM, NC, DM, and 2DM are seen to have the same values, or even lower values, of the spectral amplitude and spectral phase test parameters as the background noise. Statistically, this means that the SEE features can not be separated from narrowband Gaussian noise. No sinusoidal components are therefore expected to be found and  $T_3$  does not show any significant deviation from zero mean value.

### 6.2 The tentative BDM

From  $T_1$  in Fig. 6a we see that the tentative BDM deviates significantly from the Rayleigh distribution while in Fig. 6b,  $T_2$  shows that the spectral phase distribution cannot be distinguished from the uniform distribution. Consequently,  $H_0$

can be rejected for the tentative BDM. In Fig. 7c,  $T_3$  shows no sign of sinusoids.

Comparing the tentative BDM amplitude distribution of Fig. 5 with the DM amplitude distribution in Fig. 3, we see that the tentative BDM is more spread out than the other SEE features. It is because of this spread the test shows a deviation from the Rayleigh distribution.

An inspection of the time series (not shown here) reveals that the tentative BDM is caused by a periodic pulse of short duration with a period of 6.7 ms. It spreads over  $\pm 35$  kHz from the pump with maximum at  $\pm 30$  kHz. This structure is not present before pump turn-on but appears directly after, while the BUM and the DM are not excited until after about a second. The tentative BDM is most likely a pump transmitter induced interference, but should be investigated further.

### 6.3 The pump wave

In Figs. 6a and 6b,  $T_1$  and  $T_2$  show that the pump has a clear deviation from the Rayleigh and uniform distributions, respectively. Furthermore, in Fig. 7c  $T_3$  displays a non-zero mean value of the spectral component amplitudes. Therefore, we can conclude that the spectral amplitudes of the pump wave is Rice distributed and contain a sinusoidal plus noise.

### 6.4 Radio interferences

Figure 6a shows that most of the interferences have amplitudes which deviates from Rayleigh distributions, but in Fig. 6b only the interference at  $-95$  kHz deviates from an uniform phase distribution. This same interference is also the only one for which  $T_3$  shows presence of sinusoidal components. Therefore, the spectral amplitudes of the  $-95$  kHz interference are Rice distributed.

Even though we have modified the phases by adding the phase shift from the start of the time series, the interference at  $+85$  kHz has a phase which wraps around regularly resulting in very evenly distributed phases and therefore also a clear minimum for the phase test parameter in Fig. 6b. This interference does not show presence of any sinusoids and the spectral amplitudes cannot be Rice distributed.

The rest of the interferences also display large values of the amplitude test parameter, which excludes the possibility that they are noise-like. These interferences show uniform phases in  $T_2$  and no sign of sinusoids in  $T_3$ , making it probable that no carrier wave is present.

### 6.5 Detection of hidden signals

An interesting property of  $T_1$  can be noted for the interference at 40 kHz, which hardly is detectable in the power spectrum of Fig. 6c. This interference is almost completely hidden by the BUM in the power spectrum in Fig. 6c, but appears much clearer in the spectral amplitude test  $T_1$  in Fig. 6a. This suggests that the test  $T_1$  also can be used to detect signals which are concealed by more powerful, but noise-like,

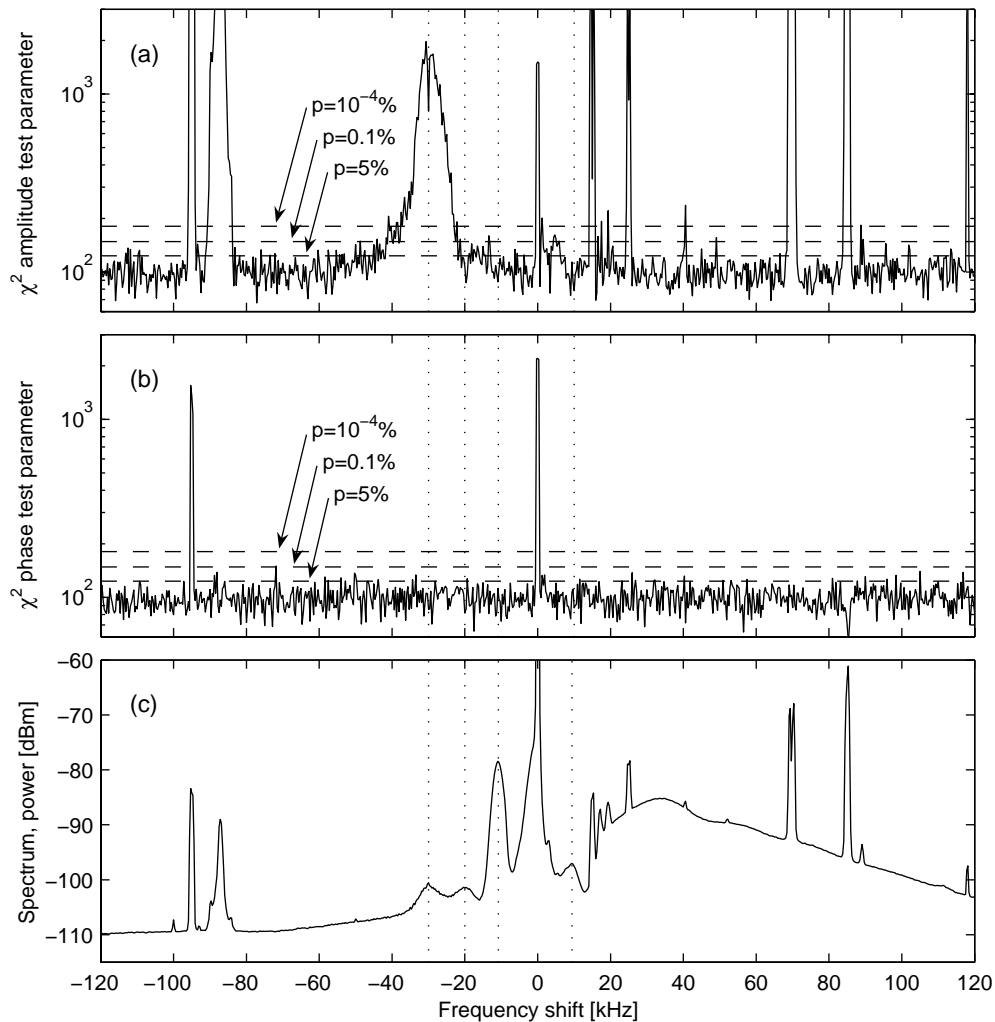


**Fig. 6.** The result of the amplitude and phase goodness-of-fit tests. Panel (a) shows the  $T_1$   $\chi^2$  spectral amplitude test parameter, panel (b) the  $T_2$   $\chi^2$  spectral phase test parameter, and panel (c) the average SEE power spectrum with vertical dotted lines marking the SEE features. The power spectrum is identical to Fig. 1. The p values of 5%, 0.1%, and  $10^{-4}\%$  are marked with the horizontal dashed lines in panels a) and b).

signals in the power spectrum. The method should also be possible to use in the opposite way to remove interferences hidden in data which are expected to be random.

### 6.6 The SEE generation process

We have found that, based on the statistical tests used here, steady-state SEE features cannot be distinguished from colored Gaussian noise. This result has implications for which processes may be involved in the generation of SEE. Now, the established explanation for several SEE-features (such as the DM) is that they are induced by parametric wave-wave processes initiated by the pump. The results of our tests are, however, not compatible with a single, isolated parametric process. This is because the waves induced in this way are necessarily coherent as long as the pump wave is

coherent, and since the radio transmitter used in our experiment is highly stable this explanation is not sufficient on its own. Our results does not, however, rule out the possibility that there could be many statistically independent parametric wave-wave interactions taking place concurrently, at various locations in the pump-ionosphere interaction region. Thus the parametric wave-wave model can be reconciled with our results, but only if we assume that there are a large ensemble of such wave-wave interactions, over both space and time, and that the induced fields superimpose incoherently at the receiver.

It should be pointed out that the statistical tests we have used here do not exclude the possibility that some, or all, of the time series of the SEE frequency component waveforms could be chaotic, since, for instance, our statistical tests did not involve higher-order (cross) moments of the time series.



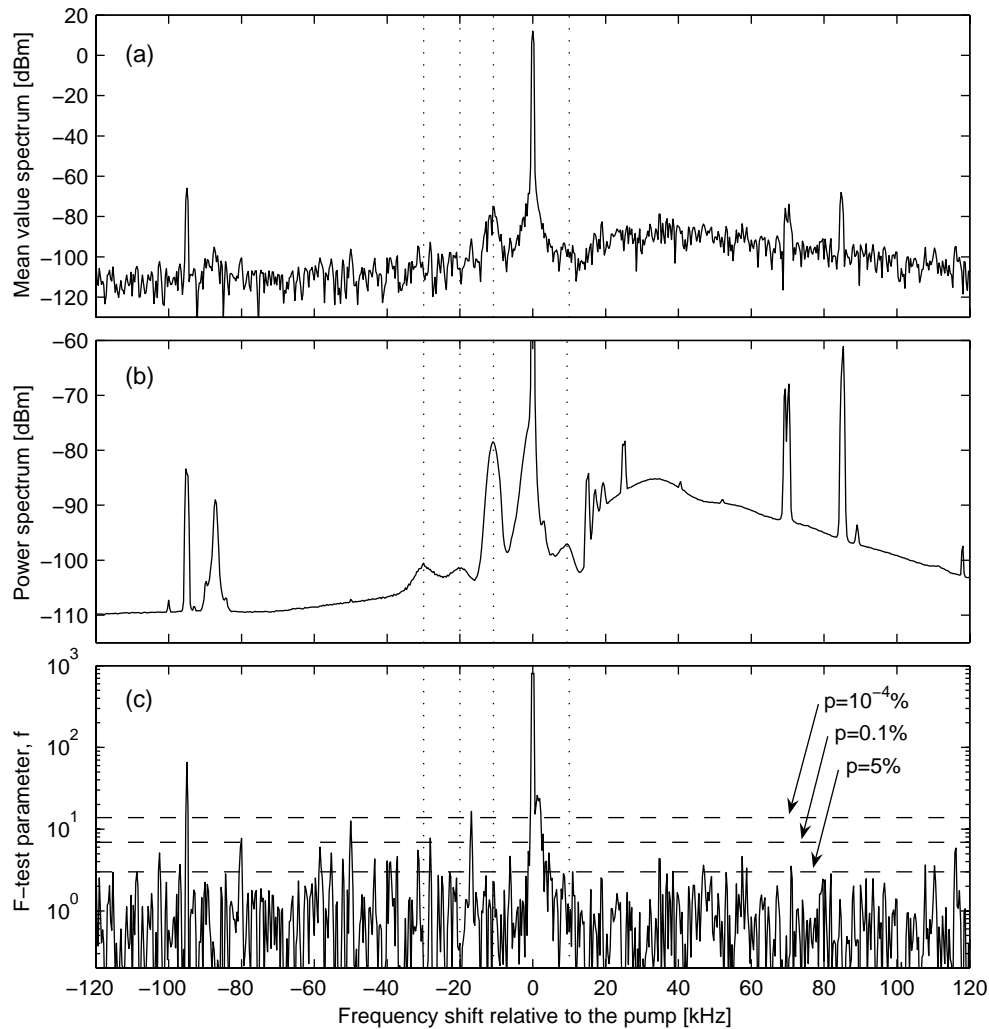


**Fig. 7.** Test  $T_3$  for sinusoidal components. Panel (a) shows the mean value spectrum (first order spectrum) according to Eq. (10) and panel (b) the power spectrum (second order spectrum) from Eq. (7). This power spectrum, with vertical dotted lines indicating the SEE features, is identical to the power spectrum in Figs. 1 and 6. In panel (c), the  $T_3$  test parameter, given by Eq. (11), is shown together with  $p$  values of 5%, 0.1%, and  $10^{-4}\%$ . The two largest peaks in panel (c) are the pump and the interference at  $-95$  kHz.

In particular this may be the case for the BUM feature, which is difficult to explain in terms of parametric wave-wave processes.

## 6.7 Remarks

A clear indication that the presented method works is given by the fact that the pump wave and the man-made interferences, which all are known to be coherent, also are indicated as coherent by the statistical tests, and that the spectral components not corresponding to any SEE features or other man-made processes all appear as noise in the tests.

The multi taper method (Percival and Walden, 1993; Thomson, 1982) could also have been used for the analysis, but that method is not optimal in this case because it is

computationally demanding to use for the large number of samples needed to obtain a satisfying result.

Expressed with respect to the sampling frequency of 320 kHz, the 1024 sample von Hann window, which was used in the analysis, has the uncertainty in time  $\Delta t=0.453$  ms and in frequency  $\Delta f=180$  Hz. This gives an uncertainty product of  $\Delta f \Delta t=0.0817$ , which can be compared with the theoretical minimum of  $1/(4\pi)=0.0796$ . Further, the time segment usage is 14% and the effective bandwidth 58%. By also implementing overlap, the usage in time can be increased, but the price to pay is that the data will contain redundant information. In this paper we have not used any overlap for the Fourier transform so all the spectral components are independent.

## 7 Conclusions

The three tests show that the pump wave and all the interferences can be clearly separated from coloured complex Gaussian noise. The pump wave has been shown to be composed of a sinusoidal plus noise and has spectral amplitudes which are Rice distributed, while only the interference at  $-95$  kHz has Rice distributed spectral amplitudes. The other interferences show no sign of sinusoidals, which indicates that carrier waves are missing.

The most important result concerns the SEE features BUM, UM, NC, DM, and 2DM, which have been shown to exhibit Rayleigh distributed spectral amplitudes and uniformly distributed spectral phases and statistically they can therefore not be separated from coloured complex Gaussian noise. This means that these SEE features cannot be the result of a single isolated coherent parametric wave-wave process. However, we cannot exclude that they may be formed as a superposition by a large number of statistically independent parametric wave-wave processes taking place at various parts of the HF-pumped ionosphere. Neither does the test give us any possibility to exclude that the amplitudes and phases of the SEE features could be chaotic. Therefore, other tests which, for example, investigate the statistics between different spectral components, may be valuable and could possibly reveal higher-order couplings or chaos.

The suggested SEE generation model with many distributed interaction regions might be tested by designing an experiment with a narrow pump lobe. A smaller part of the ionosphere would then be illuminated and for a sufficiently narrow pump lobe the SEE features may become coherent.

Here, we have only studied steady-state SEE. It may be possible that the SEE spectral features show a more coherent behaviour at early stages just after pump onset. Therefore, the statistical properties of early stage SEE should be considered for future studies.

Far from all the known SEE features were excited in the SEE experiment we have analysed. The other SEE features should also be examined with similar statistical methods. The tests could also be applied to study the statistics of naturally occurring radio emissions.

*Acknowledgements.* The authors would like to thank V. L. Frolov, S. M. Grach, M. Holz, G. P. Komrakov, T. B. Leyser, and E. N. Sergeev for having performed the measurements and collected the data used in this paper. Financial support is acknowledged from the Swedish Research Council (VR), the Swedish Royal Academy of Sciences (KVA). R. L. Karlsson also acknowledges financial support from the Advanced Instrumentation and Measurements (AIM) graduate school at Uppsala university.

Topical Editor M. Pinnock thanks two referees for their help in evaluating this paper.

## References

- Bendat, J. S. and Piersol, A. G.: Random data: Analysis and measurement procedures, 2nd ed., Wiley-Interscience, New York, 80, 1986.
- Leyser, T. B.: Stimulated electromagnetic emissions by high-frequency electromagnetic pumping of the ionospheric plasma, *Space Sci. Rev.*, 98, 223–328, 2001.
- Percival, D. B. and Walden, A. T.: Spectral Analysis for Physical Applications: multitaper and conventional univariate techniques, Cambridge University Press, Cambridge, 1993.
- Rice, S. O.: Mathematical analysis of random noise, *Bell Syst. Tech. J.*, 23, 282–332, 1944.
- Stubbe, P., Kopka, H., Thidé, B., and Derblom, H.: Stimulated Electromagnetic Emission: A New Technique to Study the Parametric Decay Instability in the Ionosphere, *J. Geophys. Res.*, 89, 7523–7536, 1984.
- Thidé: Stimulated scattering of large amplitude waves in the ionosphere: experimental results, *Phys. Scr.*, 30, 170–180, 1990.
- Thidé, B., Kopka, H., and Stubbe, P.: Observations of stimulated scattering of a strong high-frequency radio wave in the ionosphere, *Phys. Rev. Lett.*, 49, 1561–1564, 1982.
- Thomson, D. J.: Spectrum estimation and harmonic analysis, *Proc. IEEE*, 70(9), 1055–1096, 1982.
- Weiland, J. and Wilhelmsson, H.: Coherent Non-Linear Interaction of Waves in Plasmas, Pergamon Press, Oxford, 1977.
- Whitham, G. B.: Linear and nonlinear waves, John Wiley & Sons, New York, 1974.